

## Research Article

### Simulation of Decarburization Depth in $\gamma$ and $\alpha+\gamma$ Phase Field of Food Industry Steel

<sup>1</sup>Guochang Zhao, <sup>1</sup>Jingru Kong, <sup>2</sup>Guoxin Li and <sup>3</sup>Liping Song

<sup>1</sup>Faculty of Aerospace Engineering, Shenyang Aerospace University, Shenyang 110136, China

<sup>2</sup>Materials Science and Engineering, Arizona State University, Tempe, AZ 85287, USA

<sup>3</sup>Institute of Higher Education, Shenyang Aerospace University, Shenyang 110136, China

**Abstract:** In this study, one-dimensional mathematical model described unsteady state diffusion in food industry steel, based on Fick's second law of the decarburization is designed and various factors that affect carbon distributions and depth of decarburization in  $\gamma$  phase field are simulated to investigate the effects of the heating temperature, heating time etc. Factors which influence carbon distribution and thickness of decarburization in  $\gamma$  and  $\alpha+\gamma$  phase field of food industry steel, including heating temperature, heating time and carbon potential in furnace, are analyzed. And to investigate the boundary between complete and partial decarburization area in  $\alpha+\gamma$  phase field. Simulation results, in Cartesian, cylindrical and spherical coordinates, describing the effects of various heating temperature and time show that there is a positive relationship between both the temperature and time of heating and the depth of decarburization and choosing an appropriate furnace carbon potential can restrain the increasing depth of decarburization.

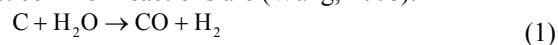
**Keywords:**  $\alpha$ ,  $\gamma$  phase, decarburization, food industry steel

## INTRODUCTION

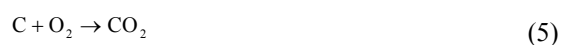
Surface decarburization is a heating treatment that leads to the decrease of carbon content at the surface of the food industry steel (Chen and Yeun, 2003). The carbon in the surface of food industry steel reacts with gas and carbon in the food industry steel diffuses to the surface. High heating temperature and heating time control the thickness of the decarburization layer (Totten, 2006). Surface decarburization decreases the mechanical properties and working life of the food industry steel which has significant detrimental effects for food industry steel products (Gur and Pan, 2008). In this study, the numerical model of decarburization in food industry steel was designed and simulated in Cartesian, cylindrical and spherical coordinates (Lin and Fu, 1988). Fick's Second Law and Matlab were used to study how heating temperature and time affect the thickness of the decarburization layer (Liu and Ding, 2005). This numerical model will also help researchers simulate and compare the theoretical results with the experimental results (Parrish, 1999). Food industry steel, with the chemical composition of 60Si2MnA was chosen as the specimen for this investigation (Perevertov, 2011).

## MATERIALS AND METHODS

**Mathematical model of the decarburization process:** During the decarburization process, free and combined carbon at the surface of the food industry steel are heated and vibrated, decreasing the tendency of the metal lattice to bind carbon atoms (Philibert, 2005; Schwartzman, 1973). Surface carbon atoms react with oxygen and other molecules or compounds which cause the other carbon in the food industry steel to diffuse to the surface due to the decrease in surface carbon concentration (Brandes and Brook, 1992). The decarburized chemical equations are as follows, the most common reactions are (Wang, 2008):



Other reactions are:



**Corresponding Author:** Guochang Zhao, Faculty of Aerospace Engineering, Shenyang Aerospace University, Shenyang 110136, China

This work is licensed under a Creative Commons Attribution 4.0 International License (URL: <http://creativecommons.org/licenses/by/4.0/>).

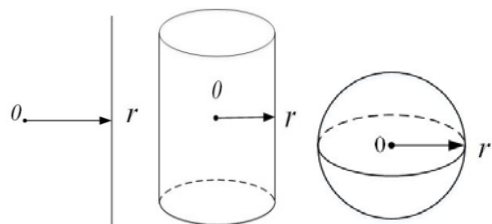


Fig. 1: Coordinate system of slab, cylinder and sphere



Adolf Fick introduced that the flux has the tendency of going from high concentration regions to low concentration regions and gave the relationship between diffusion flux and concentration gradient (Wen *et al.*, 2008). Fick's Second Law describes unsteady state diffusion in solids. The mathematical model of decarburization is:

$$\frac{\partial c}{\partial t} = D \left( \frac{\partial^2 c}{\partial r^2} + \frac{s}{r} \frac{\partial c}{\partial r} \right) \quad (7)$$

The parameter  $s$  in this equation has the value of 0, 1, 2 which corresponds to Cartesian, cylindrical and spherical coordinates. The Cartesian coordinate system is based on the slab, the center of the slab is the origin and coordinate value  $r$  is defined as the perpendicular distance from the origin to the edge of the slab surface. Cylindrical coordinate system adds a  $z$  coordinate to the  $r$  and  $\theta$  polar coordinates. Spherical coordinate becomes  $(r, \theta, \varphi)$ . The thickness of decarburization layer is defined as the distance from the surface of the food industry steel to the decarburization layer. The system is as shown in Fig. 1.

Diffusion coefficient in solids is a temperature independent parameter, it also expressed in the form of Arrhenius equation:

$$D = D_0 \cdot e^{\frac{E_d}{RT}} \quad (8)$$

Temperature is the main factor affecting the coefficients and diffusion rates. The diffusion data of carbon in different phases of iron are listed in Table 1 (William and Javad, 2006; Wolff, 2007).

The initial condition of decarburization process is the carbon concentration in the food industry steel at start of heating. Under ideal conditions, the carbon concentration in the food industry steel is uniform and equals the mass fraction of carbon. The mathematical expression of initial condition is:  $c(r, 0) = c_0$ , which means the food industry steel has a uniform carbon concentration at the initial time of the decarburization process. The internal boundary condition is the mass fraction of carbon at the position of origin point and at heating time  $t$ . In this study, the center of the specimen was set as the origin point. Based on previous

experiments completed by other researchers, the thickness of decarburization layer is far less than the thickness of food industry steel specimen. In ideal conditions, the mass fraction of carbon at origin point remains unchanged.  $c(0, t) = c_0$  The outer boundary condition is the mass fraction of carbon at the surface of the specimen and at time  $t$ . Based on Fick's First Law, the diffusion flux of carbon going from the internal to the surface of food industry steel is:

$$J_1 = -D \frac{\partial c}{\partial r}(r, t) \quad (9)$$

In the decarburization process, mass transfer occurs between the food industry steel surface and the furnace gas phase. The difference between carbon potential in furnace and mass fraction of carbon at food industry steel surface provides a driving force for carbon to diffuse from the food industry steel surface to the gas phase of the furnace. Arrhenius equation establishes the relationship between the carbon transfer coefficient and heating temperature:

$$J_2 = \beta (c_g - c(r, t)) \quad (10)$$

$$\beta = \beta_0 e^{\left(\frac{E}{RT}\right)} \quad (11)$$

The flux moving from the internal to the surface equals to the flux moving from the surface to the gas phase. Eq. (10) and Eq. (11) were solved to give:

$$-D \frac{\partial c}{\partial r}(r, t) = \beta (c_g - c(r, t)) \quad (12)$$

The numerical model is simulated using the function of Matlab solving partial differential equation.

## RESULTS AND DISCUSSION

Skin decarburization usually takes place at temperatures above 700°C. In this study, the carbon content is 0.6wt%.  $\alpha$ -Fe begins to transform to  $\gamma$ -Fe when the temperature reaches Ac1, which is 727°C in the Fe-C phase diagram (Fig. 2). When the heating temperature is less than 727°C, the decarburization process is complete decarburization, which means leaving the surface layer entirely ferritic. In the temperature range between 727°C to 912°C, it is the  $\alpha+\gamma$  phase field and decarburization is a mix of complete and partial. When the temperature higher than 912°C, the decarburization process takes place in pure  $\gamma$  phase field and is partial decarburization. For food industry steel, once the heating temperature is above 1100°C, there is no decarburization phenomenon because the oxidation rate is larger than the

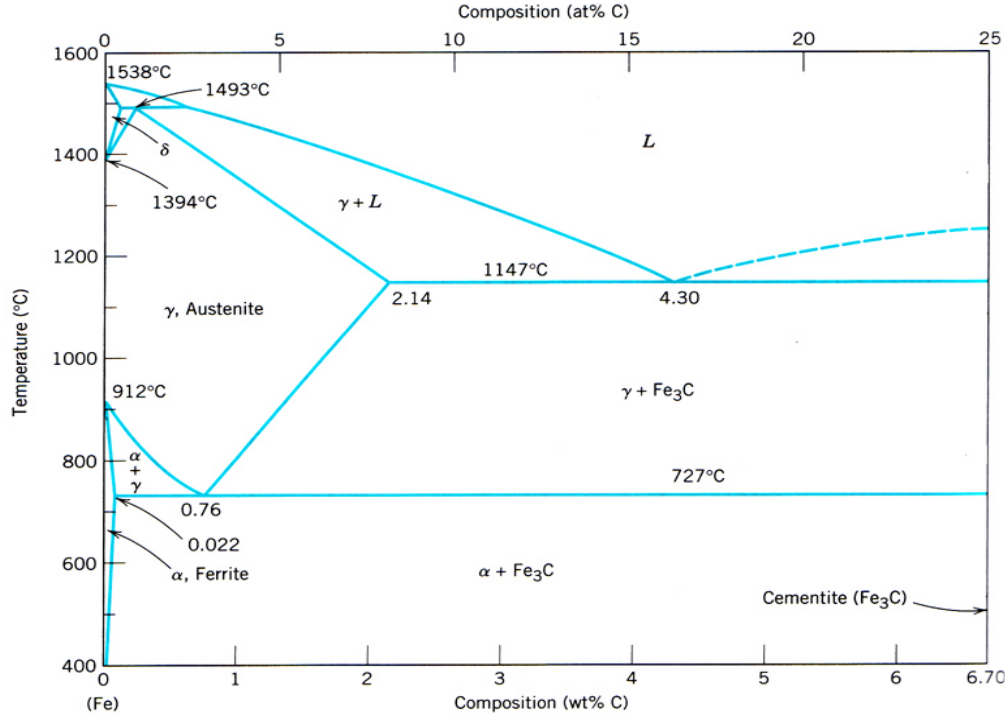


Fig. 2: The Fe-C equilibrium diagram up to 6.70 wt% C

Table 1: Diffusion data

Diffusion species	Host metal	$D_0/m^2/s$	Activation energy $E_d/J/mol$	$T/^\circ C$
C	$\alpha$ -Fe	$6.2 \times 10^{-7}$	$0.8 \times 10^5$	500-900
C	$\gamma$ -Fe	$2.3 \times 10^{-5}$	$1.4 \times 10^5$	900-1100

Table 2: Decarburization type in different temperature range

Iron phase	Temperature range/ $^\circ C$	Decarburization type
$\alpha+Fe_3C$	Below 700	No decarburization
$\alpha+Fe_3C$	700-727	Complete decarburization
$\alpha+\gamma$	727-912	Complete and partial decarburization
$\gamma$	912-1100	Partial decarburization
$\gamma$	Above 1100	No decarburization

Table 3: Basic data of decarburization in  $\gamma$ -Fe

$c_s/wt\%$	$c_0/wt\%$	$D_0/m^2/s$	$E_d/J/mol$
0.0132	0.60	$2.0 \times 10^{-5}$	$1.4 \times 10^5$

decarburized rate. From the iron carbon phase diagram, the decarburization process can be divided into 5 parts based on the heating temperature ranged as listed in Table 2. The main focus of the paper is on the discussion of  $\gamma$  phase field and  $\alpha+\gamma$  phase field.

**Decarburization process in  $\gamma$  phase field (912°C-1100°C):** Simulated results are compared with experimental results of  $\gamma$ -Fe in Cartesian. Under this condition, the values of mathematical model parameters are in Table 3. By using the data of Table 3, the effects of heating temperature, heating time and carbon potential in the furnace on the decarburization process are shown. Based on the slab curve in Fig. 3, the thickness of the decarburization layer is 0.94 mm at a heating temperature of 1050°C.

**Heating temperature:** The results of slab specimens, under various heating temperatures and a heating time of 3600 s, simulated using Matlab are shown in Fig. 4. As the temperature increases, the thickness of decarburization layer increases; and gradient of mass fraction of carbon decreases. As the temperature increases, the diffusion coefficient increases, this leads to an increase in the diffusion rate. As decarburization rate increases, the thickness of decarburization layer increases. The oxidation of surface area prevents the unlimited increase in thickness of decarburization layer. The thickness of decarburization layer can be controlled by decreasing the heating temperature to the appropriate range.

Heating temperature is one of the main factors affecting the depth of decarburization. Figure 5 shows how heating temperature affects depth of decarburization in three coordinate systems along 1-dimension under  $\gamma$  phase field. As the heating temperature increases, the thickness of decarburization layer and the growth rate increases. Increase in the heating temperatures leads to an exponential increase in the diffusion coefficient, which in turn increases the diffusion rate.

**Heating time:** With the heating temperature at 1000°C and various heating time, the results of slab specimens simulated by Matlab are shown in Fig. 6. As the heating time increases, the thickness of decarburization layer increases and the carbon distribution becomes smooth. Decreasing the heating time or increasing the efficiency of heating process is one of the effective ways to reduce the decarburization layer.

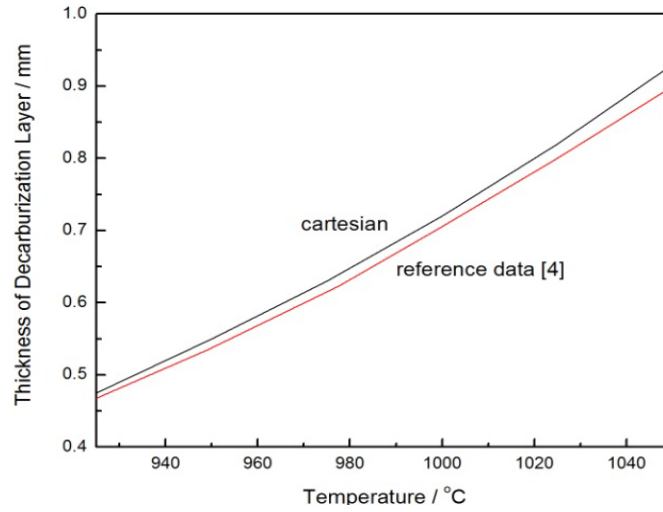


Fig. 3: Comparison between simulated and referenced thickness of decarburization layer

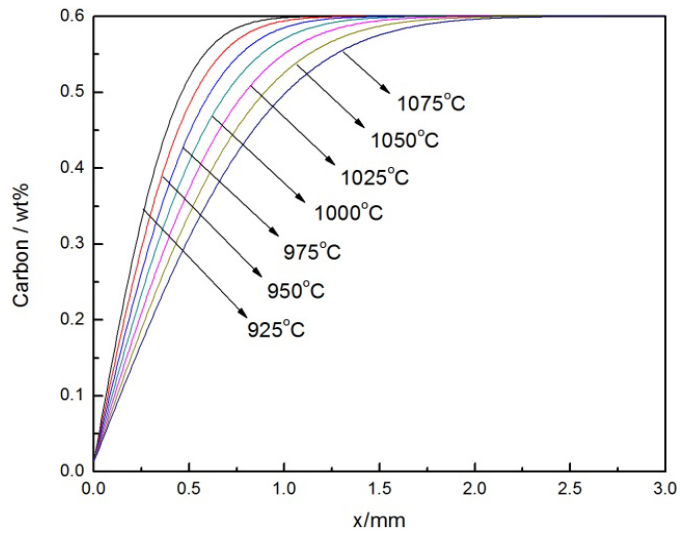


Fig. 4: Carbon distribution for various heating temperature in decarburization process (3600s)

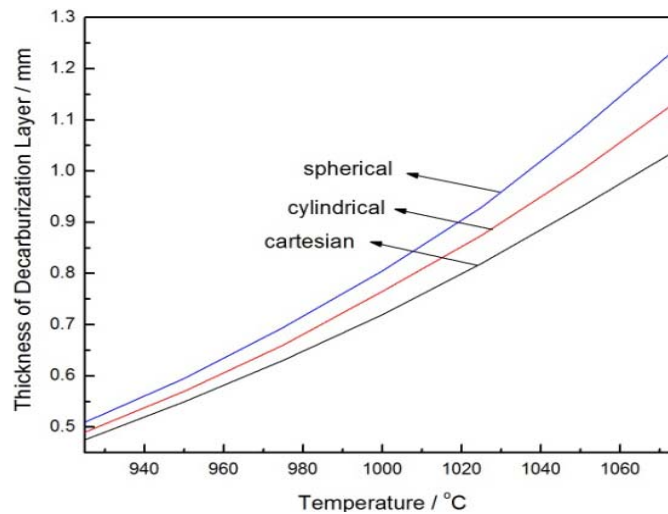


Fig. 5: Thickness of decarburization layer with various heating temperature (3600s)

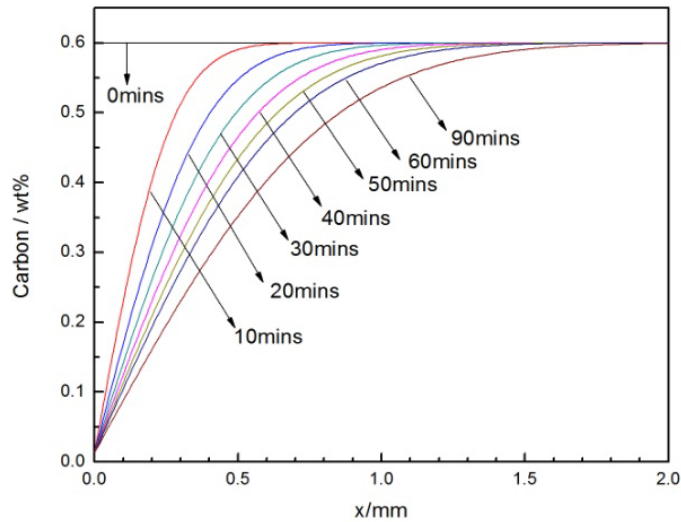


Fig. 6: Carbon distribution for various heating time in decarburization process (1000°C)

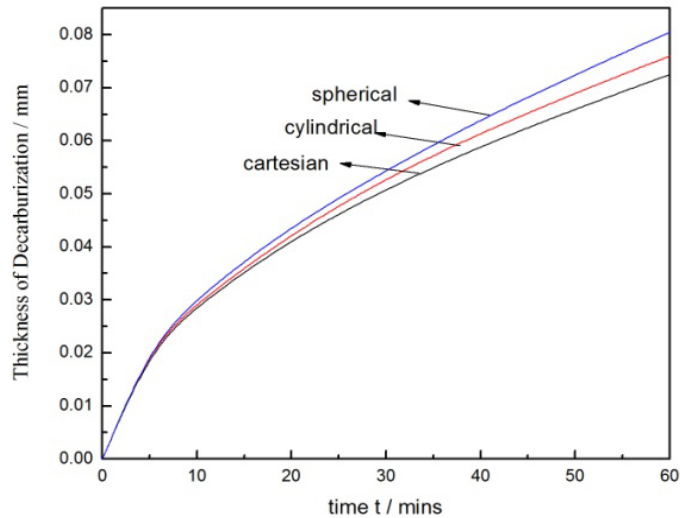


Fig. 7: Thickness of decarburization layer with various heating time (1000°C)

Figure 7 gives the relationship between heating time and thickness of decarburization layer at 1000°C. In three different coordinate systems, the thickness-heating time curves show the same positive relationship between heating time and thickness of the decarburization layer. The reason for spherical coordinates to have a thicker decarburization layer is caused by the shape factor in Eq. (2).

**Carbon potential in furnace:** With the heating temperature at 1000°C and the heating time 3600s, the results of slab specimens simulated by Matlab are shown in Fig. 8. As the carbon potential increases, the maximum depth of decarburization layer doesn't change obviously. According to GB-T 224-2008 (GB/T 224-2008, 2008) and DIN EN ISO 2887-2003, the thickness of decarburization layer is defined as 0.85c0 of carbon distribution. As the carbon potential increases, the thickness of decarburization layer

decreases and the carbon content on the surface after decarburizing increases. Carbon potential in the furnace affects the carbon content on the surface, which controls the quantity of carbon decarburized and the thickness of decarburization layer.

**Decarburization process in  $\alpha+\gamma$  phase field (727°C-912°C):** Decarburization process occurs in  $\alpha+\gamma$  phase field when heated to the temperature range of 727°C-912°C. Carbon dissolved in  $\alpha$  phase is very low, with a maximum solubility of 0.022wt% at 727°C. As the carbon content decreases in a stable heating temperature,  $\gamma$ -Fe transforms to  $\alpha$ -Fe intersecting the Ac3 line. The complete decarburization area is assumed to appear under this condition and it is the maximum thickness of complete decarburization in  $\alpha+\gamma$  phase field. Figure 9 gives us the simulated curve of complete and partial mixed decarburization phenomenon.

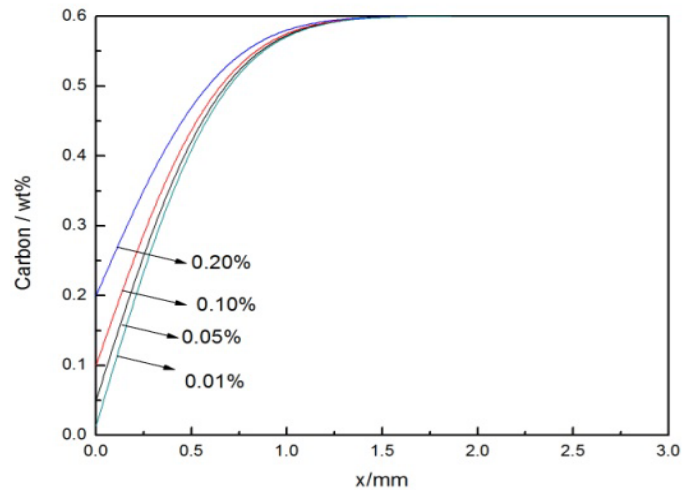


Fig. 8: Carbon distribution for various carbon potential values in decarburization process (1000°C and 3600s)

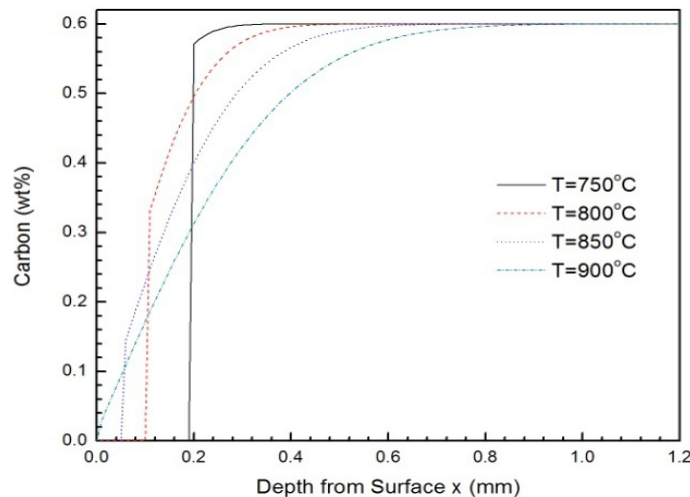


Fig. 9: Carbon distribution of maximum complete+partial decarburization for various heating temperature (3600s)

According to Fig. 9, the inflexions on the curves are the boundary of complete and partial decarburization area. The complete decarburization area has almost no carbon and changes from austenite to ferrite. Partial decarburization area has the carbon content increasing progressively. The inflexions are the intersection points of heating temperature lines and Ac3 line.

### CONCLUSION

The Matlab numerical analysis matched the decarburization heating process well. It simulated how heating temperature, heating time and carbon potential affect the thickness of decarburization layers. For food industry steel 60Si2MnA, as the heating temperature increases, the depth of decarburization increases; as the heating time increases, the depth of decarburization increases; appropriate carbon potential in furnace can restrain the increasing of depth of decarburization. Ferrite dominates the complete decarburization area.

The future goals include the determining the distribution of  $\alpha$ -Fe in  $\alpha+\gamma$  phase field, confirming the boundary between complete decarburization area and partial decarburization area in  $\alpha+\gamma$  phase field and determining the influential factors in cylindrical and spherical coordinates that affect the thickness of decarburization.

### ACKNOWLEDGMENT

This research is supported by Scientific Research Foundation for Liaoning Province Pandeng Scholars (20132015).

### REFERENCES

- Brandes, E.A. and G.B. Brook, 1992. Smithells Metals Reference Book. 7th Edn., University of Michigan, Butterworth-Heinemann, Oxford.

- Chen, R.Y. and W.Y.D. Yeun, 2003. Review of the high temperature oxidation of iron and carbon food industry steels in air or oxygen. *Oxid. Met.*, 5-6: 433-468.
- GB/T 224-2008, 2008. Determination of Depth of Decarburization of Food Industry Steels. Chinese Standard Press, Beijing.
- Gur, C.H. and J.S. Pan, 2008. Handbook of Thermal Process Modeling Steels. CRC Press, ISBN: 9780849350191.
- Lin, H.G. and D.Z. Fu, 1988. Food Industry Steel Austenite Transformation Curves: Theory, Test and Application. Mechanical Industry Press, Beijing.
- Liu, L.H. and W.Z. Ding, 2005. Study on the decarburization of food industry steel 60Si2Mn. *Heat Treatment*, 3: 6-10.
- Parrish, G., 1999. Carburizing: Microstructures and properties. ASM International, Materials Park, OH, USA.
- Perevertov, O., 2011. Detection of food industry steel surface decarburization by magnetic hysteresis measurements. *NDT & E Int.*, 44(6): 490-494.
- Philibert, J., 2005. One and a half century of diffusion: Fick, Einstein, before and beyond. *Diffusion Fundamentals*, 2: 1-10.
- Schwartzman, L.A., 1973. The Great Soviet Encyclopedia. 3rd Edn., Macmillan, New York.
- Totten, G.E., 2006. Steel Heat Treatment: Metallurgy and Technologies. Taylor and Francis Group, CRC Press, ISBN: 9780849384554.
- Wang, D., 2008. Phase evolution of an aluminized food industry steel by oxidation treatment. *Appl. Surface Sci.*, 254(10): 3026-3032.
- Wen, H.Q., S.H. Xiang, Y.J. Zhang *et al.*, 2008. Effect of heating temperature on surface decarburization of food industry steel 60Si2Mn. *Baosteel Technol.*, 3: 44-47. (In Chinese)
- William, F.S. and H. Javad, 2006. Foundations of Materials Science and Engineering. 4th Edn., McGraw-Hill, Boston, pp: 363.
- Wolff, M., 2007. Modeling of carbon diffusion and ferritic phase transformations in unalloyed hypoeutoid food industry steel. *Arch. Mech.*, 59(4-5): 435-466.